SCIENTIFIC REPORTS

OPEN

Direct formation of peritectic phase but no primary phase appearance within Ni$_{83.25}$Zr$_{16.75}$ peritectic alloy during free fall

P. Lü & H. P. Wang

Ni$_{83.25}$Zr$_{16.75}$ peritectic alloy was containerlessly solidified in a drop tube. When the droplet diameter exceeds a critical value (D_{crit}), Ni$_7$Zr$_2$ phase primarily solidifies, followed by the peritectic reaction of Ni$_7$Zr$_2$ + L → Ni$_5$Zr. Once the droplet diameter is smaller than the critical value (D_{crit}), peritectic phase Ni$_5$Zr directly solidifies from the undercooled melt by completely suppressing the nucleation and growth of Ni$_7$Zr$_2$ phase, which is ascribed to high undercooling and cooling rate. Additionally, peritectic phase Ni$_5$Zr grows equiaxially in the sample solidified in a DSC at a cooling rate of 0.167 K/s.

Peritectic reaction, in which the primary phase reacts with a liquid phase at a triple junction on cooling to produce the peritectic phase, is observed in many binary alloys systems, such as Ti-Al, Fe-Co, Fe-Ni, etc[1–3]. Peritectic reaction terminates once the primary phase is enwrapped by the peritectic phase. Then, the primary phase transforms to the peritectic phase by peritectic transformation. Due to the sluggishness of long-range solid-state diffusion, peritectic transformation could not proceed completely, leading to the existence of primary phase in the final microstructure after peritectic solidification. Recently, microstructures containing only peritectic phase with no primary phase were reported during the solidification of highly undercooled peritectic alloys, which has aroused great interest[4–9]. Wei et al.[6] reported that once the undercooling exceeds a critical value of about 220 K, peritectic phase forms directly from the metastable liquid phase by suppressing the nucleation of primary phase for Cu-70%Sn alloy, which is hyperperitectic composition. Phanikumar et al.[8] found that the microstructure is nearly phase-pure peritectic phase when Fe-25%Ge peritectic alloy is undercooled up to 110 K using electromagnetic levitation technique, in which the primary phase is a solid solute phase of α-Fe. Löser et al.[9] reported that beyond a critical undercooling, the equilibrium solidification can be replaced by the direct growth of peritectic phase for Co$_{75}$Si$_{25}$ peritectic alloy. Although some study results have been reported, fundamental and deep understanding of different aspects of peritectic solidification is still poor. These investigations mainly focus on the effect of undercooling on phase selection and microstructure evolution. It is not clear how the peritectic phase could directly form from liquid alloys, especially for some complicated peritectic alloys, for example, both the primary phase and the peritectic phase are intermetallic compounds.

The Ni-Zr binary alloy system contains abundant metallic compounds and amorphous alloys, which have been studied extensively[10–16]. However, most works concentrate on the atomic structure and glass forming ability. Ni$_{83.25}$Zr$_{16.75}$ alloy is a typical peritectic composition in Ni-Zr binary alloy system. The primary phase Ni$_7$Zr$_2$ and peritectic phase Ni$_5$Zr are both intermetallic compounds. Phase selections between primary phase and peritectic phase have great influence on the final solidified microstructures, which directly relate to the materials characteristics. Therefore, the objective of this work is to investigate effects of undercooling and cooling rate on phase selection and microstructure evolution of Ni$_{83.25}$Zr$_{16.75}$ peritectic alloy by a 3 m drop tube. Meanwhile, the effect of cooling rate on peritectic growth is also studied.

Results and Discussion

Figure 1 shows the left part of Ni-Zr binary phase diagram[17], in which the studied Ni$_{83.25}$Zr$_{16.75}$ peritectic alloy is marked with an arrow. As can been seen, the solidification of Ni$_{83.25}$Zr$_{16.75}$ peritectic alloy starts with the formation

MOE key Laboratory of Space Applied Physics and Chemistry, Department of Applied Physics, Northwestern Polytechnical University, Xi'an 710072, P. R. China. Correspondence and requests for materials should be addressed to H.P.W. (email: hpwang@nwpu.edu.cn)
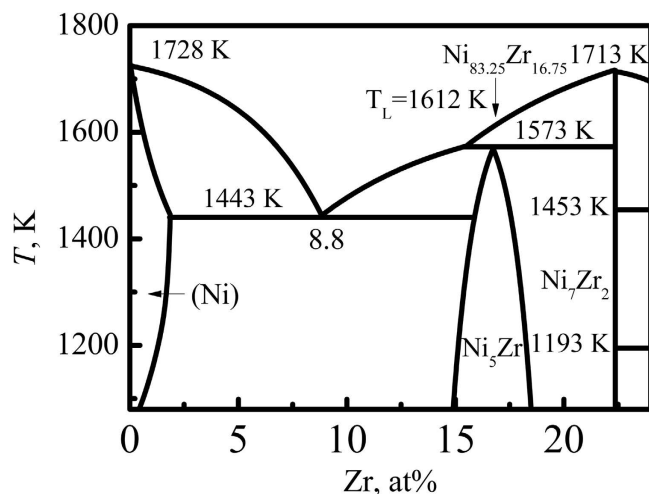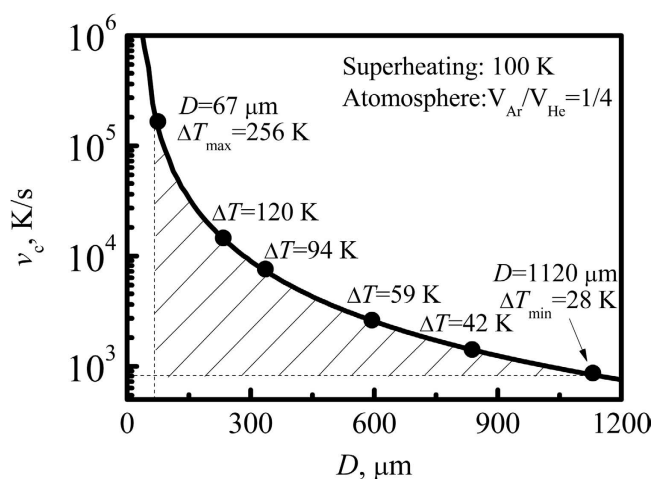
Figure 1. The left part of Ni-Zr binary phase diagram[17].

Figure 2. Calculated average cooling rate and undercooling versus droplet diameter.

Parameter	Value
Peritectic composition, C_0 (at.%)	16.75
Peritectic temperature, T_p (K)	1612
Heat of fusion, ΔH (J mol^{-1})	9176
Heat capacity, C_p (J/mol/K)	36.84
Mass density, ρ (Kg m^{-3})	8092
Stefan-Boltzmann constant, σ_{SB} (W cm^{-2} K^{-4})	5.67×10^{-12}
Surface emissivity, ε_h	0.45

Table 1. Physical parameters of Ni$_{83.25}$Zr$_{16.75}$ peritectic alloy[20].

of primary Ni$_7$Zr$_2$ phase and a peritectic reaction of Ni$_7$Zr$_2$ + $L \rightarrow$ Ni$_5$Zr occurs at 1573 K under the equilibrium condition. 100% peritectic phase is obtained when peritectic solidification is accomplished.

Drop tube processing has the advantage to achieve high cooling rate and undercooling, which is quite suitable to investigate the phase selection. However, it is hard to measure and record the temperature experimentally due to the short time of free fall. Under this condition, heat transfer theory[18,19] is applied to calculate the cooling rate and undercooling of droplets. The calculated results are shown in Fig. 2, and Table 1 lists the physical parameters used in the calculation[20]. It can be seen that the cooling rate and undercooling strongly depend on droplet diameter.

Figure 3 illustrates the solidified microstructures of Ni$_{83.25}$Zr$_{16.75}$ peritectic droplets with different diameters, in which the primary phase Ni$_7$Zr$_2$ and the peritectic product Ni$_5$Zr have been marked. In the droplet of
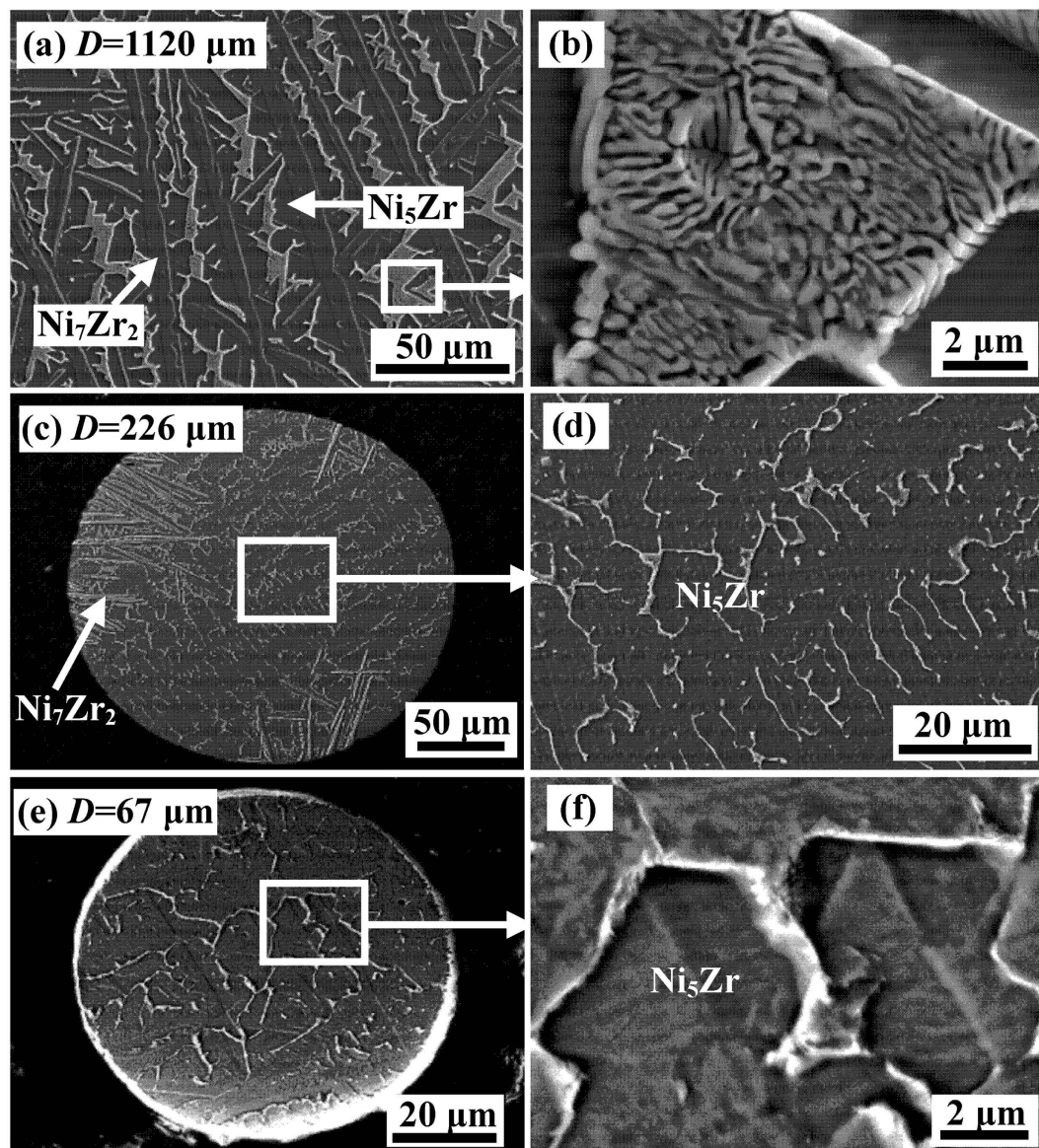
Figure 3. Solidified microstuctures of $Ni_{83.25}Zr_{16.75}$ peritectic droplets with different diameters.
(**a,b**) $D = 1120\,\mu m$; (**c, d**) $D = 226\,\mu m$; (**e,f**) $D = 67\,\mu m$.

1120 μm, the solidified microstructures are composed of primary Ni_7Zr_2 dendrites, peritectic phase Ni_5Zr and inter-dendritic eutectic, as show in Fig. 3(a). Evidently, the primary phase Ni_7Zr_2 is characterized by coarse, developed dendrites and surrounded by peritectic phase Ni_5Zr. Figure 3(b) is the enlargement of inter-dendritic eutectic microstructure in Fig. 3(a). It must be noticed that there is no any prediction of eutectic transformation for this composition according to the equilibrium phase diagram. This will be discussed in the following parts. With the decrease of droplet diameter, the refinement and fragment of primary Ni_7Zr_2 dendrites occur. When the droplet diameters decrease to 226 μm, the microstructure consists of two regions, as presented in Fig. 3(c). Clearly, one is primary Ni_7Zr_2 dendrites surrounded by peritectic phase Ni_5Zr, which locate at the rim of the droplet. The other is Ni_5Zr phase with no primary phase Ni_7Zr_2 locating at the center of the droplet, as illustrated in Fig. 3(d). The peritectic phase Ni_5Zr is the predominant phase. When the droplet diameter is very small like 67 μm, only peritectic phase Ni_5Zr grows within the whole droplet and no Ni_7Zr_2 dendrites can be observed, as presented in Fig. 3(e,f).

According to Kerr and Kurz's description[21], peritectic solidification consists of two processes, one is the solidification of primary phase and the other is the growth of peritectic phase. Meanwhile, three stages have been identified during a peritectic growth process, namely, peritectic reaction, peritectic transformation, and direct solidification of the peritectic phase. Different solidification pathway of $Ni_{83.25}Zr_{16.75}$ peritectic droplets can be concluded based on the solidified microstructure presented in Fig. 3. In the droplets whose diameters are large, the primary phase Ni_7Zr_2 is expected to nucleate at temperature below the liquidus temperature and grows into the manner of dendrites. With the decrease of droplets temperature, the peritectic phase Ni_5Zr starts to nucleate
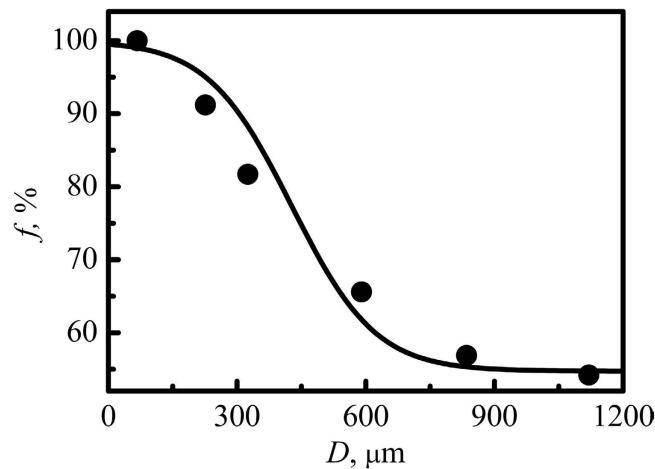
Figure 4. Average volume fractions of peritectic phase Ni₅Zr versus droplet diameter.

at the surface of primary phase Ni_7Zr_2 when the temperature below the peritectic temperature. The requirement of peritectic reaction, which is primary phase, peritectic phase and liquid must be in contact with each other at a triple junction, is satisfied after the nucleation of peritectic phase Ni_5Zr. Then, peritectic reaction starts and peritectic phase Ni_5Zr grows along the surface of primary Ni_7Zr_2 dendrites to form a thin layer. Since peritectic reaction is controlled by short-range atomic diffusion in the liquid ahead of primary Ni_7Zr_2 dendrites and peritectic phase Ni_5Zr, it is able to accomplish rapidly at the initial stage of the peritectic growth process[21]. Once the primary Ni_7Zr_2 dendrites are enveloped by the peritectic phase, the primary phase and liquid are separated by the peritectic phase, which results in the disappearance of the triple junction and the termination of peritectic reaction. After peritectic reaction, the peritectic phase Ni_5Zr grows into the primary Ni_7Zr_2 dendrites by peritectic transformation and into the liquid by direct solidification. Peritectic transformation is controlled by long-range solid-state diffusion and the cooling rate in drop tube processing is always high, leading that peritectic transformation could hardly take place. Therefore, the primary Ni_7Zr_2 dendrites are retained in the microstructure, as illustrated in Fig. 3(a). Simultaneously, peritectic phase Ni_5Zr grows into the liquid by direct solidification, which results in the deviation of residual liquid composition. As a consequence, the residual liquid solidifies as eutectic when the temperature decreases below the eutectic temperature, as illustrated in Fig. 3(b). The morphology in Fig. 3(b) is characterized by lamellar eutectic structure, where the bright one is (Ni) phase and the other is Ni_5Zr phase.

With the decrease of droplet diameters, the possibility for a droplet to contain heterogeneous nucleation site is reduced. Therefore, droplets with small diameters can obtain high undercoolings. The enhancement of undercooling greatly promotes the nucleate rate of primary phase Ni_7Zr_2, which results in the refinement of primary Ni_7Zr_2 dendrites. Meanwhile, the release of latent heat remelts the primary phase leading to the fragment of Ni_7Zr_2 dendrites. As a result, the contact area between primary Ni_7Zr_2 dendrites and liquid increases. This apparently promotes the peritectic reaction and thus more primary Ni_7Zr_2 dendrites are decomposed. Similarly, residual liquid directly solidifies as Ni_5Zr phase and a small amount of eutectic successively. According to the above analysis, it can be speculated that the volume fractions of peritectic phase increase with the decrease of droplet diameters. In order to validate the conclusion, the volume fractions of peritectic phase have been measured, which is illustrated in Fig. 4. Apparently, with the decrease of droplet diameters, the volume fraction of peritectic phase Ni_5Zr increases, which is consistent with the speculation.

When the droplet diameter is 226 μm, the microstructure consists of only a small amount of primary Ni_7Zr_2 dendrites near the rim of droplet and predominant Ni_5Zr phase without any Ni_7Zr_2 phase in the center, as presented in Fig. 3(c,d). The possibility for the formation of such a microstructure is that the peritectic phase Ni_5Zr homogeneously nucleates at the center of the undercooled droplet and then starts to grow. Unfortunately, the peritectic phase Ni_5Zr grows into a faceted way, the growth velocity of which is sluggish. The release of crystallization heat leads to a rise of temperature and a decrease of interface undercooling of Ni_5Zr phase. Therefore, the growth of peritectic phase Ni_5Zr will be terminated. At this small undercooling, the primary phase Ni_7Zr_2 is preferred to nucleate and grow. Following that, peritectic reaction takes place when the temperature drops below the peritectic temperature T_P. As for $Ni_{83.25}Zr_{16.75}$ peritectic alloy, the liquidus temperature of Ni_7Zr_2 phase is larger than that of Ni_5Zr phase about 39 K, which leads to a high driving force for the nucleation of Ni_7Zr_2 phase. Therefore, Ni_7Zr_2 phase is preferred to nucleate. However, this is not the case under high undercooling condition. From a thermodynamic point of view, the change in Gibbs free energy, dG, determines which phase is thermodynamically stable at given temperature and pressure, expressed as

$$dG = V \cdot dP - S \cdot dT + \sum_i \mu_i \cdot dN_i$$

(1)

Equation (1) relates the change in Gibbs free energy to the sum of products of volume V, entropy S, chemical potential μ_i and the changes of pressure dP, temperature dT and number of particles dN_i[22]. Chemical potential is the driving force of atom diffusion in a concentration field.
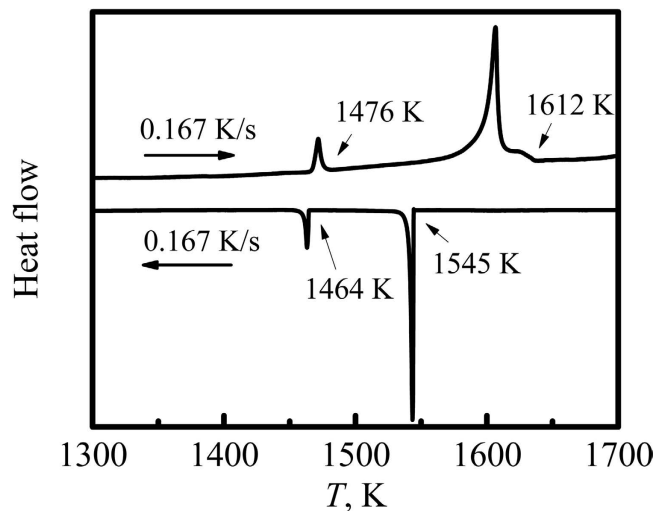
Figure 5. DSC curve of $Ni_{83.25}Zr_{16.75}$ peritectic alloy.

If the droplet is undercooled below the peritectic temperature T_p, the formation of a new phase is determined by the competitive nucleation of Ni_7Zr_2 phase and Ni_5Zr phase. Clusters are the initial stage of nucleation. The formation of clusters needs atoms diffuse and attach together. When the attachment rate of atoms to the cluster is larger than the detachment rate of atoms to the same cluster, this cluster can form stable within the undercooled droplet. The concentration of droplet is the same as that of peritectic phase Ni_5Zr. As a consequence, large chemical potential is required to form the clusters of Ni_7Zr_2 phase compared with the formation of Ni_5Zr clusters, resulting in large Gibbs free energy barrier to nucleation of Ni_7Zr_2 phase. Thus, compared with the nucleation of Ni_5Zr phase, high undercooling is required to nucleate the Ni_7Zr_2 phase. Fortunately, the undercooling of Ni_7Zr_2 phase ΔT is always larger than the undercooling of Ni_5Zr phase ΔT_p about 39 K, which is beneficial to the nucleation of Ni_7Zr_2 phase. Therefore, Ni_7Zr_2 phase is still preferred to nucleate when the droplet is undercooled just below the peritectic temperature T_p. However, the $\Delta T/\Delta T_p$ ratio is decreased with the further increase of undercooling ΔT, leading to the disappearance of the advantage of the nucleation of Ni_7Zr_2 phase. The undercooling is up to 120 K for the droplet whose diameter is 226 μm. Hence, peritectic phase Ni_5Zr may primarily nucleates from the undercooled droplet when the droplet diameter is 226 μm.

With the further decease of droplet diameter, the peritectic phase Ni_5Zr is more preferred to nucleate. A heat flux from the melt to the surroundings is required during the solidification process, which changes the free energies and therefore the relative thermodynamic stability, of the phases present[23]. Actually, the heat flux from the melt to the surrounding is absolutely dominated by the cooling rate. In the droplets whose diameter is 67 μm, the cooling rate is up to 1.8×10^5 K/s, which leads that the crystallization heat is rapidly transformed to the surroundings during the peritectic growth. Therefore, the peritectic Ni_5Zr phase can continually grow, resulting in the formation of phase-pure Ni_5Zr microstructure, as shown in Fig. 3(e–f). The EDS analysis demonstrates that it is peritectic phase Ni_5Zr which contains about 81 at% Ni and 19 at% Zr. This indicates that high undercooling and cooling rate may totally suppress the formation of Ni_7Zr_2 phase and results in the directly nucleation and growth of peritectic phase Ni_5Zr from the undercooled melt. Besides, the critical diameter for obtaining phase-pure Ni_5Zr microstructure is in the range of 226 to 67 μm.

In order to further investigate the effects of cooling rates on peritectic growth, DSC experiment was employed to perform a comparative analysis. 20 mg of $Ni_{83.25}Zr_{16.75}$ samples was completely melted by heating to 1723 K and then solidified at a cooling rate of 0.167 K/s. The DSC curves are shown in Fig. 5, in which the upper curve is the heating curve and the other is the cooling curve. It can be seen that there are two peaks during the solidification, which represent the solidification of primary phase Ni_7Zr_2 and the growth of peritectic phase Ni_5Zr, respectively. The solidified sample has a undercooling of 67 K and the microstructure is illustrated in Fig. 6(a). Obviously, the microstructure consists of predominate peritectic phase Ni_5Zr and a small amount of primary phase Ni_7Zr_2. Besides, a majority of peritectic phase Ni_5Zr grows equiaxially. This indicates that peritectic transformation proceeds for a relatively long time duo to the low cooling rate in the DSC. Figure 6(b) shows the microstructure solidified in the drop tube at the similar undercooling level but with a high cooling rate of about 2.8×10^3 K/s. The microstructure are composed of primary phase Ni_7Zr_2, peritectic phase Ni_5Zr and eutectic, which shows completely different morphology compared with that in Fig. 6(a). The Ni_5Zr phase exhibits faceted morphology, indicating that peritectic phase grows mainly by peritectic reaction and direct solidification under high cooling rate condition. This reveals a different peritectic growth mechanism under different cooling rate condition.

Conclusion

In summary, $Ni_{83.25}Zr_{16.75}$ peritectic alloy was rapidly solidified in a 3 m drop tube. The microstructure evolution with the decrease of droplet diameter is investigated. For large droplets, solidified microstructures are composed of primary Ni_7Zr_2 dendrites, peritectic phase Ni_5Zr and eutectic. The competitive nucleation and growth between Ni_7Zr_2 phase and Ni_5Zr phase become intensive as droplet diameter decreases. The solidified microstructure consists of only peritectic phase Ni_5Zr once the droplet diameter less than a critical value, D_{crit}, which is determined
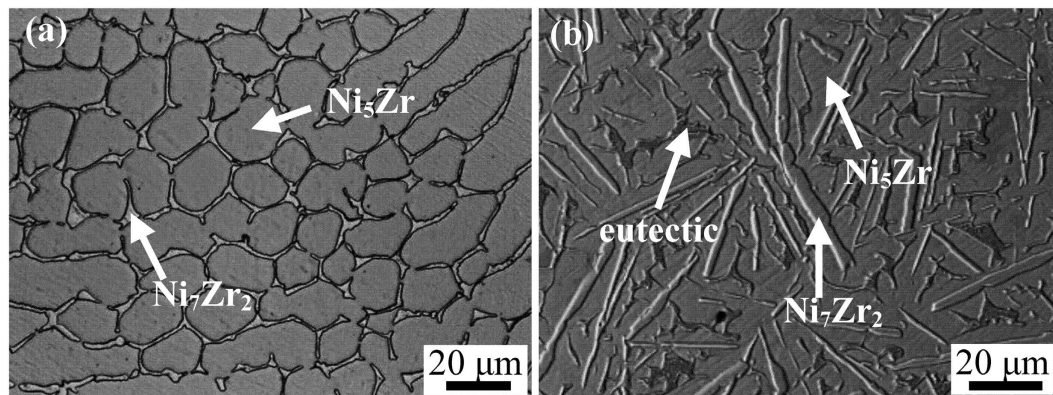
Figure 6. Microstructures of Ni$_{83.25}$Zr$_{16.75}$ sample solidified under different cooling rate. (**a**) cooling rate of 0.167 K/s in the DSC; (**b**) cooling rate of 2.8×10^3 K/s in the drop tube.

in the range of 226 to 67 μm. For $D > D_{crit}$, Ni$_7$Zr$_2$ phase primarily solidified, followed by the peritectic reaction of Ni$_7$Zr$_2$ + L → Ni$_5$Zr. For $D < D_{crit}$, peritectic Ni$_5$Zr phase directly solidifies from the undercooled melt by completely suppressing the nucleation and growth of Ni$_7$Zr$_2$ phase, which is ascribed to high undercooling and cooling rate. Ni$_{83.25}$Zr$_{16.75}$ sample solidified in the DSC contains no eutectic and the morphologies of peritectic phase Ni$_5$Zr is equiaxial, indicating that peritectic phase grows mainly by peritectic reaction and peritectic transformation under low cooling rate condition.

Experimental Details

Containerless rapid solidification of Ni$_{83.25}$Zr$_{16.75}$ peritectic alloy was performed in a 3 m drop tube. The master alloy samples were prepared by 99.99% pure Ni and 99.9% pure Zr mixtures in an argon atmosphere, and each of samples has a mass of 1.0 g. When the experiment began, the sample was placed in a silica tube, which has a Φ0.2 mm orifice at bottom and was installed at the top of 3 m drop tube. The drop tube was evacuated to 10^{-5} Pa and backfilled with 20% Ar and 80% He gas mixture to 1 atm. After melted by induction heating, the sample was ejected out from the orifice and dispersed into many fine droplets by exerting argon gas flow. The droplets were solidified rapidly in a containerless state during free fall. After that, the droplets were collected and sieved into several groups according to their sizes. The solidified samples were analyzed by FEI Sirion SEM and Oxford INCA 300 EDS.

References

1. Clemens, H. & Mayer, S. Design, processing, microstructure, properties, and applications of advanced intermetallic TiAl alloys. *Adv. Eng. Mater.* **15,** 191–215 (2013).
2. Liu, N. *et al.* Solidification behaviour of undercooled peritectic Fe$_{81.68}$Co$_{18.32}$ alloy. *J. Alloys Comp.* **485,** L12–L15 (2009).
3. Chen, Y. Z. *et al.* Suppression of peritectic reaction in the undercooled peritectic Fe–Ni melts. *Scripta Mater.* **57,** 779–782 (2007).
4. Peng, P. *et al.* Influence of solutal convection on solute distribution of melt during preparation of directionally solidified Sn–36at.% Ni peritectic alloy. *Int. J. Heat Mass Tran.* **84,** 73–79 (2015).
5. Griesser, S., Reid, M., Bernhard, C. & Dippenaar, R. Diffusional constrained crystal nucleation during peritectic phase transitions. *Acta Mater.* **67,** 335–341 (2014).
6. Zhai, W. & Wei, B. Direct nucleation and growth of peritectic phase induced by substantial undercooling condition. *Mater. Lett.* **108,** 145–148 (2013).
7. Asta, M. *et al.* Solidification microstructures and solid-state parallels: Recent developments, future directions. *Acta Mater.* **57,** 941–971 (2009).
8. Phanikumar, G. *et al.* Solidification of undercooled peritectic Fe–Ge alloy. *Acta Mater.* **53,** 3591–3600 (2005).
9. Löser, W., Leonhardt, M., Lindenkreuz, H. G. & Arnold, B. Phase selection in undercooled binary peritectic alloy melts. *Mater. Sci. Eng. A* **375,** 534–539 (2003).
10. Cao, Y. F. *et al.* Laser shock peening on Zr-based bulk metallic glass and its effect on plasticity: experiment and modeling. *Sci. Rep.* **5,** 10798 (2014).
11. Du, J., Wen, B., Melnik, R. & Kawazoe, Y. First-principles studies on structural, mechanical, thermodynamic and electronic properties of Ni–Zr intermetallic compounds. *Intermetallics.* **54,** 110–119 (2014).
12. Turnow, H., Wendrock, H., Menzel, S., Gemming, T. & Eckert, J. Synthesis and characterization of amorphous Ni–Zr thin films. *Thin Solid Films* **561,** 48–52 (2014).
13. Georgarakis, K. *et al.* On the atomic structure of Zr–Ni and Zr–Ni–Al metallic glasses. *J. Appl. Phys.* **108,** 023514 (2010).
14. Holland-Moritz, D. *et al.* Structure and dynamics of liquid Ni$_{36}$Zr$_{64}$ studied by neutron scattering. *Phys. Rev. B* **79,** 064204 (2009).
15. Hao, S. G. *et al.* Experimental and ab initio structural studies of liquid Zr$_2$Ni. *Phys. Rev. B* **79,** 104206 (2009).
16. Banerjee, S., Savalia, R. T. & Dey, G. K. Glass formation and crystallisation in rapidly solidified zirconium alloys. *Mater. Sci. Eng. A* **304,** 26–33 (2001).
17. Massalski, T. B., Okamoto, H., Subramanian, P. R. & Kacprzak, L. *Binary alloy phase diagram* Vol. 3, 1249 (ASM International, 1990).
18. Adkins, N. & Tsakiropoulos, P. Design of powder metallurgy aluminium alloys for applications at elevated temperatures Part 1 Microstructure of high pressure gas atomized powders. *Mater. Sci. and Technol.* **7,** 334–340 (1991).
19. Lee, E.-S. & Ahn, S. Solidification progress and heat transfer analysis of gas-atomized alloy droplets during spray forming. *Acta Metall. Mater.* **42,** 3231–3243 (1994).
20. Brandes, E. A. & Brook, G. B. *Smithells metals reference book* 7th edn, Ch. 14, 1–43 (London, 1992).
21. Kerr, H. W. & Kurz, W. Solidification of peritectic alloys. *Int. Mater. Rev.* **41,** 129–164 (1996).
22. Müller, I. *A history of thermodynamics—the doctrine of energy and entropy* (Springer Verlag, Berlin, 2007).
23. Kurz, W. & Fisher, D. J. *Fundamentals of solidification* 3rd edn, Ch. 2, 21–22 (Switzerland, 1992).

Author Contributions

P.L. and H.P.W. designed the experiments. P.L. carried out the experiments and wrote the paper. H.P.W. revised this paper.

Additional Information